Eur Biophys J (2005) 34: 1041–1048
DOI 10.1007/s00249-005-0489-5

ARTICLE

L. Cristofolini · M. P. Fontana · F. Serra · A. Fasano
P. Riccio · O. Konovalov

Microstructural analysis of the effects of incorporation of myelin basic protein in phospholipid layers

Received: 2 February 2005 / Revised: 7 April 2005 / Accepted: 4 May 2005 / Published online: 26 May 2005

Abstract We report an X-ray reflectivity study on the effects of adsorption of myelin basic protein (MBP) on Langmuir monolayers and on deposited Langmuir–Schaefer multilayers of the phospholipid dipalmitoyl phosphatidylglycerol (DPPG). We provide for the first time, direct microscopic evidence on the destructuring effects of MBP leading to plasticity of the DPPG layers supporting commonly accepted models of the stabilizing role of MBP in the myelin membrane. We also show how protein adsorption onto the layer is determined both by electrostatic and nonspecific hydrophobic interactions.

Keywords Myelin basic protein · X-ray reflectivity · Langmuir–Blodgett

Introduction

Myelin basic protein (MBP) is a major component of the myelin sheath, both in the central nervous system (CNS) and in the peripheral nervous systems (Martenson 1992; Harauz et al. 2004). It is believed to be the main agent in the formation and maintenance of integrity of CNS myelin (Boggs and Moscarello 1982; Riccio et al. 1986). Several reports indicate that it contains epitopes for experimental autoimmune encephalomyelitis (Ohler et al. 2004), a pathology which mimics multiple sclerosis. Recent clinical studies on the effects of MBP in multiple sclerosis patients have been published (Bielekova et al. 2000). MBP belongs to the class of intrinsically unstructured proteins (IUP), and the unraveling of its structure is still a major unsolved problem in modern structural biology. It is established that it has a substantial random coil conformation in aqueous solution (Gow and Smith 1989; Smith 1992), and that it has some coherent secondary structure when added to a lipid environment (Beniac et al. 1997), or when it is purified with detergents in the lipid-bound form (Polverini et al. 1999; Haas et al. 2004). The intrinsic disorder of MBP when it is not associated to lipids is deemed essential to its biological function, but apart from this little is known about the actual microscopic mechanisms of the roles of MBP in normal and pathological cases. In particular, the relative weight of noncovalent interactions, mainly electrostatic and hydrophobic, and their roles in determining the morphology and mechanical properties of the myelin membrane have been the subject of extensive studies, which indicate the active presence of both (Mueller et al. 1999, 2000; Bates et al. 2003; Boggs et al. 1981a). Experimental evidence suggests that MBP plays an important role in linking two opposing cytoplasmic faces of myelin membranes, as it is shown by the dilation of the coding gene in shiverer mutant mice (Roach et al. 1985), but does not seem to be so crucial in keeping together the extracellular faces of two compact membranes (Kirschner and Ganser 1980). Recent computer simulations give some specific ideas as to the special conformation of MBP, which seems to be more adequate for this role (Bates and Harauz 2003).

L. Cristofolini · M. P. Fontana · F. Serra
Dipartmento di Fisica e Istituto Nazionale
per la Fisica della Materia, Universita' di Parma,
Parco Area delle Scienze 7a, 43100 Parma, Italy

A. Fasano
Dipartimento di Biochimica e Biologia Molecolare,
Universita' di Bari, Via Orabona 4, 70126 Bari, Italy

P. Riccio
Dipartimento di Biologia, Difesa, Biotecnologie Agro-Forestali,
Universita' della Basilicata, Campus di Macchia Romana,
85100 Potenza, Italy

O. Konovalov
European Synchrotron Radiation Facility,
Avenue des Martyrs, Grenoble, France

L. Cristofolini (✉) · M. P. Fontana
Istituto Nazionale per la Fisica della Materia,
Centro Ricerca e Sviluppo SOFT, Rome, Italy
E-mail: cristofolini@fis.unipr.it

Furthermore, adsorption studies of MBP onto phospholipid (PL) monolayers at the air–water interface using sensitive but macroscopic techniques, such as quartz crystal microgravimetry and null-ellipsometry, clearly indicate intercalation of the protein into the layer both for charged and for neutral PLs (Facci et al. 2000; Polverini et al. 2003). The main difference in behavior seems to be related to the total extrusion of MBP from the neutral PL dipalmitoyl phosphatidylcholine layer at high surface pressure (30 mN m^{-1}), whereas for the negatively charged dipalmitoyl phosphatidylserine the extrusion at high compression leads to the formation of a proteolipid complex. This result has clear implications for electrostatic and excluded-volume interactions in determining how MBP influences the morphology, structure and mechanical properties of the PL layers.

In this paper, we follow up on our previous work (Facci et al. 2000; Polverini et al. 2003) and present a microscopic study of the effects of MBP adsorption onto monolayers and multilayers of the negatively charged dipalmitoyl phosphatidylglycerol (DPPG), one of the most studied PLs in this context (Boggs et al. 1981b). We used synchrotron radiation X-ray reflectivity (XRR) to obtain information on the layer morphology, thickness and structure, and its changes. An XRR study of MBP adsorption on different PL multilayers deposited from a $ZnCl_2$ subphase has been published (Haas et al. 1998). The structuring effect due to the presence of the Zn ions was demonstrated, resulting in well-ordered multilayers with MBP located between the lipid head groups of the individual bilayers, which were also shown to contain water molecules. In this work, we chose to study a system closer to the physiological environment, hence the choices of DPPG and of a pure-water subphase. Moreover, our reflectivity data explore twice the exchanged momentum range reported in Haas et al. (1998), hence allowing a more complete and detailed structural analysis. Furthermore, we studied the reflectivity from DPPG monolayers at the air–water interface, observing a spectacular destructuring effect due to the MBP interaction with the monolayer, yielding for the first time direct microscopic proof of the often hypothesized fluidification effect of MBP on PL layers.

Experimental

Chemicals and samples

MBP was purified in the water-soluble, lipid-free form from bovine brain according to established procedures (Deibler et al. 1972, 1984). The protein concentration was determined using the Bio-Rad Bradford reagent (Bio-Rad Laboratories, Hercules, CA, USA) and a microassay procedure. The MBP was used as a standard, using the molar extinction coefficient 10,300 M^{-1} at 276.4 nm (Liebes et al. 1975). The DPPG was obtained from Sigma–Aldrich (Milan, Italy) and was used without further purification.

Reflectivity setup

The XRR curves were measured at ESRF (Grenoble) using the Troika 2 (ID10B) beamline. The incident wavelength was 1.385 Å for the multilayers and 1.566 Å for the Langmuir monolayers; the angular position of the goniometer could be controlled with an accuracy of 0.01 mrad. In order to avoid saturation effects at the small reflectivity angles we used standard attenuators on the incident beam (aluminum foils with different thickness, ranging from 1.1 to 0.1 mm). The true reflectivity was separated from X-ray diffuse scattering by taking rocking curves and/or off-specular scans, and terminating the scan when the reflectivity became confused with the diffuse background. At very small angles (much below the critical angle for total reflection) a minor geometric correction was applied in order to account for the beam footprint being larger than the actual length of the sample, thus implying that only a fraction of the incident beam was intercepted and reflected by the sample. Typically, the beam had a vertical size of 50 μm, while the sample length was 20 mm. Such correction was then needed in the angular range from $\theta = 0$–$0.14°$, while the critical angle for silicon is at about $\theta = 0.37°$ at our wavelength. This experimental setup and procedure allowed us to obtain XRR scans up to $Q_z = 0.6$ $Å^{-1}$. Details can be found in Konovalov et al. (2002, 2004).

Langmuir films

We studied DPPG as a monolayer formed at the air–water interface, and as a deposited multilayer. For the monolayer XRR study, a custom-made shallow, single moveable barrier Langmuir trough (dimensions 170×438×3 mm^3) was placed on an active antivibration table. The surface pressure was measured using a Wilhelmy balance, while the barrier position and surface pressure were controlled by ESRF electronics (SPEC), which provide a software interface for the R&K electronic system (Riegler & Kirstein). The trough was sealed and filled with helium. About 150 μl of a solution of DPPG (0.63 mM either in pure chloroform or in a chloroform/methanol/water mixture, 65:15:4 in volume) was spread either on a pure-water subphase or on a subphase containing MBP (1.43 mg l^{-1}). The surface pressure was monitored upon compression with a Wilhelmy balance while performing the XRR scans. In Fig. 1, we show a typical isotherm recorded at room temperature for the DPPG Langmuir monolayer; in the same figure we also show the target surface pressures used in this work. For the multilayer deposition, the DPPG monolayer at the air–water interface was prepared as already described, using a KSV5000 trough (KSV Instruments, CT, USA). The multilayers were deposited using the Langmuir–Schaefer (LS) technique (Roberts 1990) upon an untreated silicon substrate, covered by its native oxide. The LS (horizontal dipping) technique is particularly suitable for high-viscosity

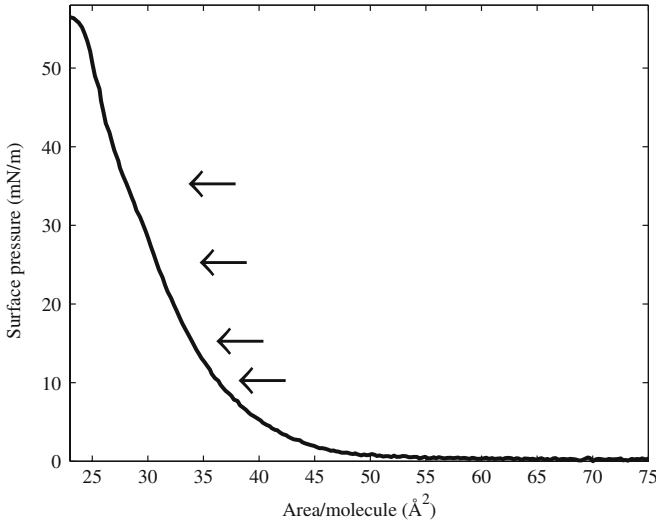

Fig. 1 Isotherm for a pure dipalmitoyl phosphatidylglycerol (*DPPG*) Langmuir monolayer, obtained after spreading a 0.63 mM solution of DPPG in a chloroform/methanol/water mixture (65:15:4 in volume) on a pure-water subphase. The *arrows* mark the values of the surface pressure at which the experiments were performed (see text for details)

monolayers at the air–water interface and yielded homogenous, high-quality deposited layers. Three samples were analyzed: one was made of ten layers deposited at 35 mN m^{-1} surface pressure; two were made of four layers, respectively, deposited at 25 and 35 mN m^{-1} pressures. The XRR curves were taken before and after dipping each sample for 15 min in an aqueous solution of 5×10^{-8} M MBP. Previous data on MBP adsorption kinetics (Facci et al. 2000) indicated that 15 min was sufficient for the adsorption to be essentially completed. A control measure was also done on a sample dipped in pure water (e.g., without MBP) for the same time.

Data analysis

The XRR data were analyzed both with our own software and with the program PARRATT (C. Braun, Parrat32 Software for Reflectivity, HMI, Berlin, 1999), which calculates theoretical reflectivity curves according to the so-called Parratt recursive approach (Parratt 1954; Daillant and Gibaud 1999). In this method one calculates the transmission and reflection Fresnel coefficients at each interface, starting from the approximation of independent smooth layers. In order to reproduce the reflectivity curve of a real multilayer, a structured model of independent layers, each with uniform electron density, has to be provided. The roughness of real layers is accounted for using the Névot–Croce approximation (Nevot and Croce 1980), which implies scaling of the reflectivity at the interface between layers a and b by the factor $\exp(-2k_a k_b \sigma^2)$, σ being the roughness root-mean-square value, and k_a and k_b representing the z-component of the wavevector for layers a and b, respectively.

Results

Multilayers

There are distinct differences between the reflectivity curves of the samples before and after their interaction with MBP, as shown in Fig. 2, where the reflected intensity is plotted against the vertical component of the exchanged momentum Q_z, which is related to the reflection angle θ and to the wavelength λ of the incident radiation by $Q_z = 4\pi/\lambda \sin\theta$. We immediately note a systematic shift of the curve minima towards smaller values and a general reduction of the contrast between minima and maxima. The control measure allows us to

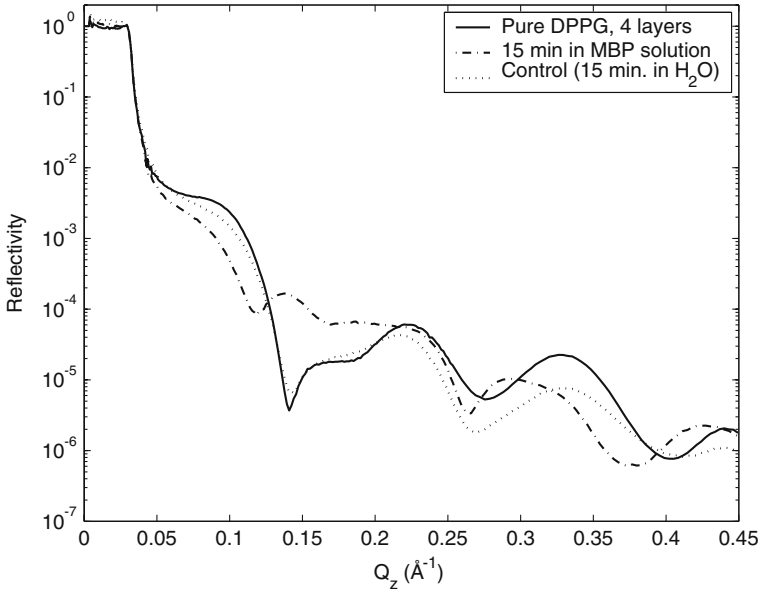

Fig. 2 Reflectivity curves for a four-layer sample deposited at 25 mN m^{-1} surface pressure. The *thick black line* represents data for phospholipids before their interaction with myelin basic protein (*MBP*); the *dashed line* represents data for the same sample after its immersion for 15 min in an MBP solution; the *dotted line* shows reflectivity of a control measure made to evaluate water–lipid interaction effects. All the curves are properly normalized in order to consider some system geometrical factors

exclude the possibility that these differences are due to the interaction of water with the PLs. However, the small but noticeable differences of the pattern after incubation in pure water indicate that water exposure slightly affects multilayer structure. This observation is in agreement with previously reported data on a different set of PLs (Riccio et al. 1986; Haas et al. 1998). In order to fit these data, and, first of all, the ones concerning noninteracting PL samples, we first chose to represent each layer as two different slabs with uniform electron density, one related to the alkyl chains and the other one to the polar head groups: this model is well known in the literature and is often used for lipid layers (Kjaer et al. 1989; Haas et al. 1998; Harper et al. 2000; Majewski et al. 2001). The relative positions of these head and tail layers give information about the LS film structure: from our analysis of the reflectivity from lipid-only films, this turns out to be a Y-structure, implying a folding of the monolayer during deposition or a recrystallization thereafter, both of which are not uncommon (Schwartz 1997).

The more important features of our model are:

- The presence of a first high-density layer, representing the polar heads lying on the substrate, implying a Y-structured film.
- Progressive reduction of electron density for the polar head group region from the first layer on silicon to the last layer exposed to air.
- For the ten-layer sample, introduction of a thick amorphous layer on the surface: for this layer, the electron density was chosen at an intermediate value between the polar head group and the hydrophobic tail electron density.

This suggests that the first layer deposited upon the silicon substrate is quite rough, because of the deposition process. As more layers are added by subsequent deposition, the film structure becomes less well defined, finally leading *after a few layers* to an almost completely amorphous mixture of PL head and tail groups. A similar phenomenon was also observed in LS films of polymeric side chain azobenzene molecules (Cristofolini et al. 2002). For the four-layer samples, this situation was best represented as a progressive reduction of the head group electron density; for the ten-layer sample this modification was not enough, and it was necessary to introduce the rough amorphous layer to abolish the distinction between head and tail layers near the film surface.

In Fig. 3, we report the data and relative fits for two pure DPPG multilayers, namely four layers deposited at 35 mN m^{-1} and ten layers at the same pressure. In the insets of the two panels of the same figure, the electron density profiles obtained by the fitting procedures are reported. We remark the good-quality fits ($\chi^2 = 0.99$ and 1.4 for the four-layer and ten-layer films, respectively) up to large momentum values $Q_z = 0.45$ Å^{-1}. As already stated, this extends by a factor of two the Q_z range explored for similar PLs (Haas et al. 1998).

Exposure of pristine DPPG multilayers to MBP resulted in major changes in the reflectivity curves of both the four-layer and the ten-layer samples (Fig. 4). In

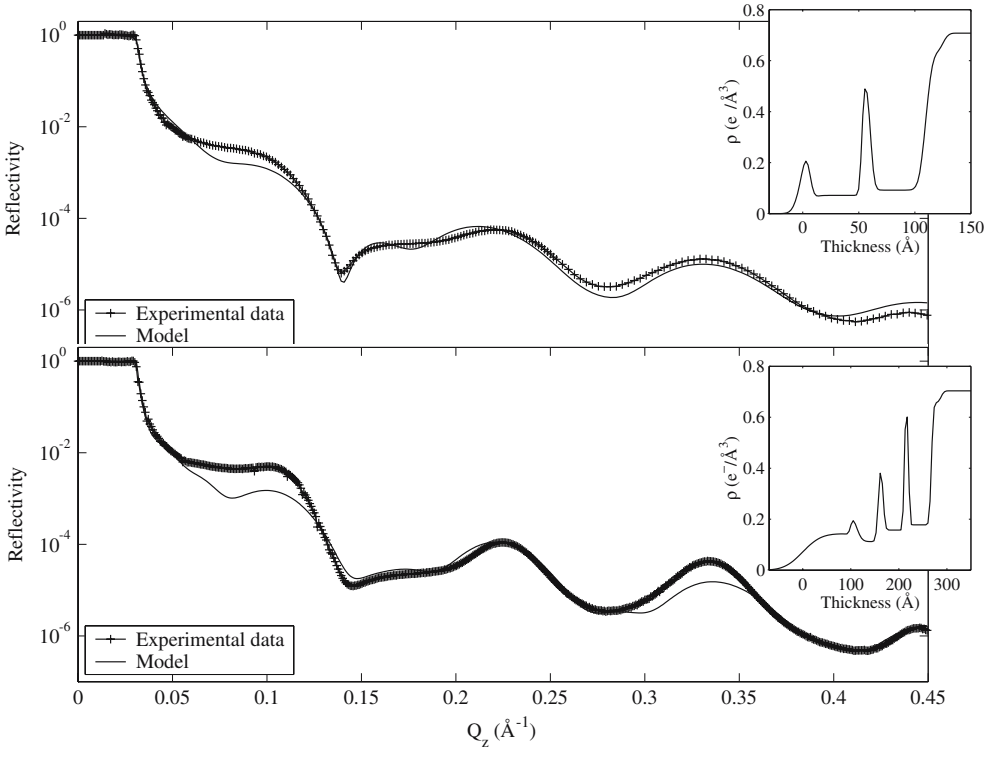

Fig. 3 *Top* Experimental reflectivity curve (*crosses*) and the best fit (*black line*) for a sample consisting of four layers of DPPG deposited at a surface pressure of 35 mN m^{-1} as a dry film before interaction with MBP. In the *inset*, the electron density profile that was used for the calculation of the fitted curve is shown. *Bottom* Experimental reflectivity curve (*crosses*) and the best fit (*black line*) for a sample consisting of ten layers of DPPG deposited at a surface pressure of 35 mN m^{-1} as a dry film before interaction with MBP. In the *inset*, the electronic density profile corresponding to the fitted curve is shown

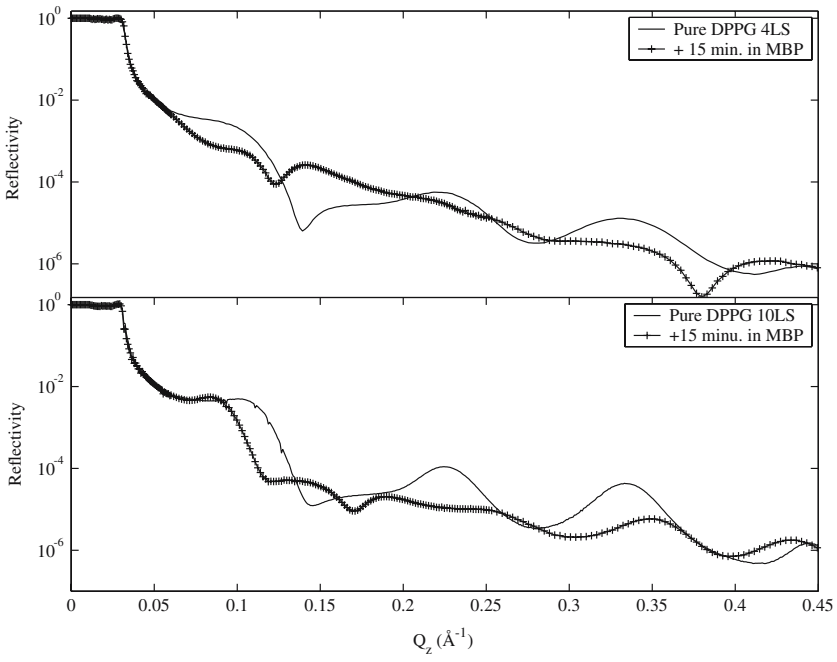

Fig. 4 Reflectivity data for samples consisting of four layers (*top*) and ten layers (*bottom*) as a dry film before (*black line*) and after (*crosses*) their interaction for 15 min in an MBP solution (see text for details). As in Fig. 2, it is possible to notice the destructuring effect and the minima shift

order to fit these data, it was necessary to introduce a large destructuring effect in the model (Fig. 5). The shift of the position of the minima in the reflectivity curve was reproduced by an expansion of the polar head region, whose thickness increases from 7.6(1) to 12.9(1) Å. The first PL bilayer is reproduced by a model very similar to that employed for the unexposed sample [i.e., alkyl chain electron density 0.10(1) e Å^{-3}, and polar head electron density 0.55(1) e Å^{-3}], while the second bilayer is reproduced by an unstructured layer with average electron density of 0.22(1) e Å^{-3}. This shows (1) that the protein interacts more strongly with the outmost layers, which is quite reasonable, and (2) that the protein does not spread uniformly inside the bilayer, but instead chooses specific parts of it, as the expansion of the polar head region suggests.

The overall quality of these fits ($\chi^2 = 2.9$) is not as good as for the ones shown for noninteracting multilayers. The main reason may be the intrinsic inhomogeneity of the layers. This explanation is reasonable if we think that protein adsorption breaks the layer homogeneity and every attempt to describe it with global parameters for electron density and roughness becomes a rough approximation.

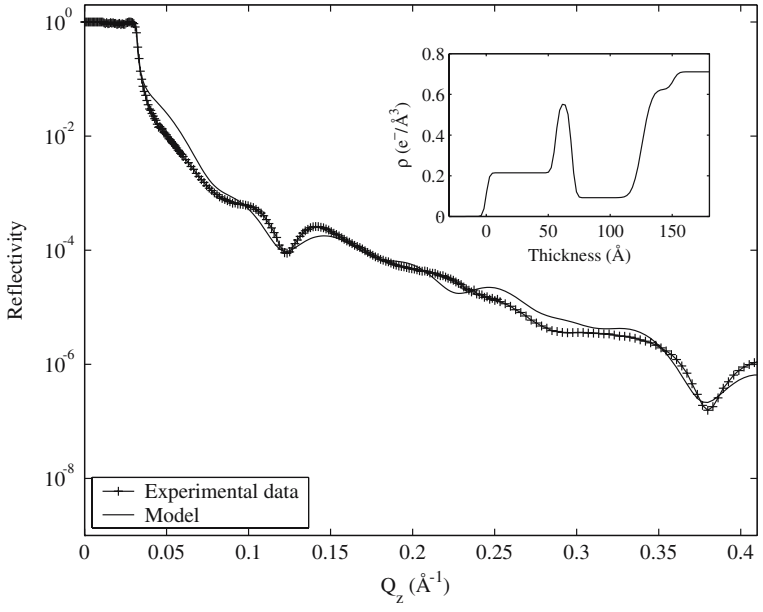

Fig. 5 Experimental reflectivity curve (*crosses*) and the best fit (*black line*) for a sample consisting of four layers of DPPG deposited at a surface pressure of 35 mN m^{-1} after interaction with MBP. In the *inset*, the electron density profile corresponding to the fitted curve is shown

Monolayers on water surface

We also measured the reflectivity of Langmuir monolayers of the same PL (DPPG) both on a pure-water subphase and on an MBP-containing subphase, as a function of lateral pressure at $\Pi = 10$, 25 and 35 mN m^{-1}.

In Fig. 6, we report the reflectivity curves, scaled by the fourth power of the exchanged momentum, measured for pure DPPG at surface pressures of 10, 25 and 35 mN m^{-1}. As for the deposited multilayers, the data could be easily fitted by the model made up of two slabs. As shown in the inset of Fig. 6, where we show for simplicity only the profile for the monolayer at $\Pi = 35$ mN m^{-1}, the polar head groups sit on the water surface and are characterized by an electron density higher than that for pure water, and above them are located the alkyl tails, characterized by a lower electron density (Graf et al. 2002). Here the quality of the fits is excellent, as shown by the near indistinguishability between the data and relative fitting curve for all three samples. As the surface pressure is increased, the position of the first minimum in the reflectivity of pure DPPG films shifts towards lower Q_z values; correspondingly in our PARRAT fit of the whole reflectivity curve, the total film thickness increases from 25.7 Å ($\Pi = 10$ mN m^{-1}) to 26.5 Å ($\Pi = 25$ mN m^{-1}) and to 27.8 Å ($\Pi = 35$ mN m^{-1}). This implies an average reduction of the molecular tilt angle as the surface pressure is increased, which is not uncommon (Kaganer et al. 1999). A detailed study also by grazing incidence diffraction would be needed to better determine the structure.

Whereas the pure DPPG on the water subphase yields a well-structured, and precisely fit, layer, the addition of MBP dramatically changes the scenario. In Fig. 7, we report the reflectivity curves measured for monolayers of DPPG exposed to MBP at different pressures ($\Pi = 10$ and 35 mN m^{-1}) compared with the corresponding curves measured for pristine PL monolayers. We immediately notice that at low pressure ($\Pi = 10$ mN m^{-1}) the reflectivity curve becomes featureless, as the minimum at 0.2 Å^{-1} disappears, with a pattern very similar to that of pure water. Thus, MBP adsorption at the interface effectively destroys the ordered structure of the monolayer, perhaps by inducing large roughness, as suggested also by the fact that if we try to fit these data, we find the self-contradictory result of a thickness which is of the same order of magnitude as the roughness parameter, which is another way of stating that the film is utterly destroyed by the presence of MBP. This behavior confirms previous results on MBP adsorption on PL membranes which were interpreted as indicating the induction of a surface undulation (Ohler et al. 2004). Whatever the origin, the resulting observed reflectivity is very similar to that of a bare water surface, the only difference being a small increase in the surface roughness (from $\sigma = 2$ to $\sigma = 3$ Å arising from capillary waves on bare water, to $\sigma = 4$ Å in our model).

As the surface pressure is increased to 35 mN m^{-1}, a similar phenomenon is observed; however, the reflectivity curve after MBP exposure retains some form of structuring, with a shallow minimum surviving around $Q_z = 0.22$ Å^{-1}. This residual structure seems to coincide in space scale to the structure reported for MBP–PL complexes in solution by small-angle X-ray scattering (Haas et al. 2004). We also checked the reproducibility of the reflectivity curve with time, which does not show any major time evolution at least up to 3 h after the film compression. This result indicates that, within this time frame, there is no radiation damage or structural rearrangement. Moreover, we checked the stability by comparing monolayers formed on a subphase containing MBP against monolayers formed on a

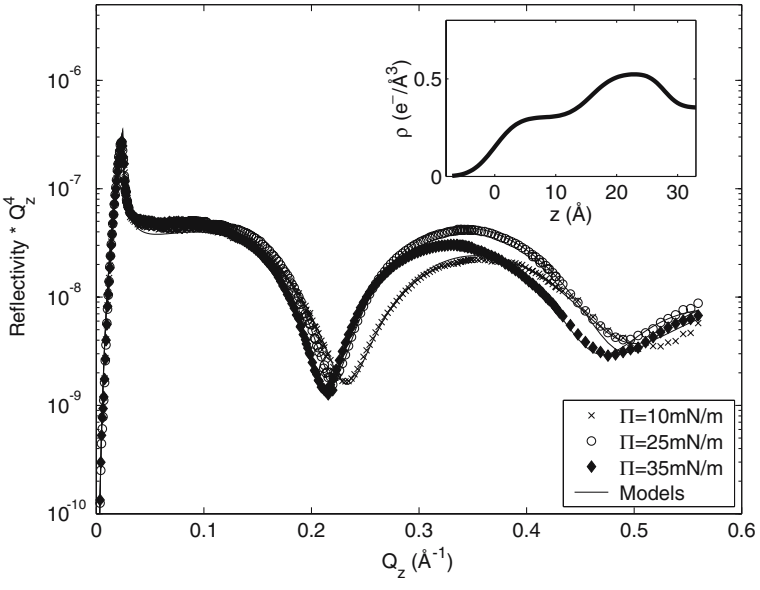

Fig. 6 Scaled reflectivity curves measured for pure DPPG Langmuir films at three different surface pressures together with the corresponding reflectivity profiles (lines almost indistinguishable from the experimental data) calculated with the model described in the text. *Inset* The electron density profile corresponding to the model that provides the best fit to the data for $\Pi = 35$ mN m^{-1}. The total film thickness corresponds to the position of the rightmost inflection point in the profile

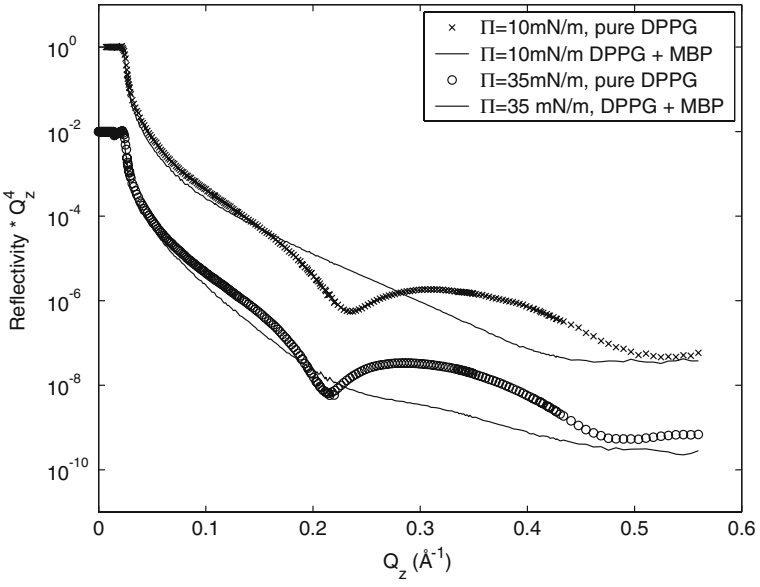

Fig. 7 Reflectivity curves measured for Langmuir monolayers of DPPG exposed to MBP at $\Pi = 10$ mN m^{-1} (*top curves*) and at $\Pi = 35$ mN m^{-1} (*bottom curves*, data are shifted down 2 orders of magnitude for clarity) compared with the corresponding curves measured for pristine phospholipid monolayers (*thick lines*)

pure-water subphase and subsequently exposed to MBP only after film lateral compression. In both cases, we obtained substantially identical results. In this case then, the interaction with MBP does not completely destroy the ordered PL film structure, although it certainly makes it less definite.

Discussion

We begin by discussing the spectacular effect of MBP on the DPPG monolayer at the air–water interface. The adsorption of the protein simply destroys whatever structural regularity the monolayer may have had, especially at a surface pressure of 10 mN m^{-1}. It is difficult to devise a structural model for the monolayer after adsorption, since there is no visible structure. Since the PL molecule cannot change its morphology too dramatically, there must be strong heterogeneity in the local environments of the PL tails, i.e., the chains are strongly disordered in conformation and orientation, resulting in a very rough layer. However, it is also possible that the monolayer breaks up and collapses; the present situation prevents any definite conclusion, however, the most likely explanation is that MBP intercalates within the PL layer, drastically increasing the film roughness and thus effectively suppressing its reflectivity. The effect seems to be less strong in the more compact monolayer at $\Pi = 35$ mN m^{-1}. This result is reasonable, since the more tightly bound chains may make it more difficult for the protein to disrupt the PL layer morphology.

We can conclude that the XRR data from Langmuir monolayers of DPPG support the previously proposed model of interaction (Riccio et al. 1986), in which the electrostatic interaction taking place between polar head groups and charged residues is the origin of the attraction and intercalation of MBP within the PL layer, at least at low surface pressure. Upon compression, partial extrusion of the protein takes place, with parts of the denatured protein still bound to the monolayer, which retains roughly its overall structure. Clearly, on the macroscopic scale, all these phenomena translate into a strong increase in monolayer plasticity.

This conclusion is confirmed by the data on solid multilayers. The mechanism we propose for MBP adsorption may support the model according to which MBP works as a glue for adjacent bilayers of the myelin sheath, as also confirmed in recent work (Hu et al. 2004) which, using force measurements and scanning microscopy, suggests that MBP acts as a lipid coupler between bilayers and as a lipid "hole filler" through noncovalent, mainly electrostatic and hydrophobic interactions. In fact, our reflectivity data provide microscopic confirmation of a large body of results and conjectures leading to the mechanism that the protein binds to polar head groups of adjacent bilayers and forms a bridge between them through polar or electrostatic attraction.

This mode of interaction is made possible by the IUP character of MBP, which gives it the necessary flexibility to unravel and adapt its partially ordered structure to the PL environment. In particular, the MBP-induced plasticity of the single monolayer can help explain the role of MBP in stabilizing and repairing the myelin membrane.

Difficulties with fitting some of our data may be explained if the homogeneous layer description for the polar head regions becomes very rough, as protein–lipid interaction creates, according to our explanation, a zone with polar head groups and MBP altogether. Since MBP randomly distributes through these regions, it is not possible to refine the model with further structuring of these layers, but it is more reasonable to use an average value of electron density. This approximation, of course, makes data-fitting less accurate; however, we chose to pursue qualitative, but physically clear, modeling,

instead of adding more parameters to obtain a nicer looking, but perhaps less informative, result.

References

Bates IR, Harauz G (2003). Molecular dynamics exposes alpha-helices in myelin basic protein. J Mol Model 5:290–297

Bates IR, Boggs JM, Feix JB, Harauz G (2003) Membrane-anchoring and charge effects in the interaction of myelin basic protein with lipid bilayers studied by site-directed spin labeling. J Biol Chem 278:29041–29047

Beniac DR, Luckevich MD, Czarnota GJ, Tompkins TA, Ridsdale RA, Ottensmeyer FP, Moscarello MA, Harauz G (1997) Three-dimensional structure of myelin basic protein. I. Reconstruction via angular reconstitution of randomly oriented single particles. J Biol Chem 272:4261–4268

Bielekova B, Goodwin B, Richert N, Cortese I, Kondo T, Afshar G, Gran B, Eaton J, Antel J, Frank JA, McFarland HF, Martin R (2000) Encephalitogenic potential of the myelin basic protein peptide (amino acids 83–99) in multiple sclerosis: results of a phase II clinical trial with an altered peptide ligand. Nat Med 6:1167–1175. Erratum in: Nat Med (2000) 6:1412

Boggs JM, Moscarello MA (1982) Structural organization of myelin: role of lipid–protein interaction determined in model system. In: Jost PC, Griffith OH (eds) Lipid–protein interactions vol 2. Wiley, New York, pp 1–51

Boggs JM, Wood DD, Moscarello MA (1981a) Hydrophobic and electrostatic interactions of myelin basic protein with lipid. Participation of N-terminal and C-terminal portions. Biochemistry 20:1065–1073

Boggs JM, Stamp D, Moscarello MA (1981b) Interaction of myelin basic protein with dipalmitoylphosphatidylglycerol: dependence on the lipid phase and investigation of a metastable state. Biochemistry 20:6066–6072

Cristofolini L, Fontana MP, Berzina T, Konovalov O (2002) Molecular relaxation and microscopic structure of multilayers and superlattices of a photosensitive liquid-crystalline polymer. Phys Rev E 66:041801

Daillant J, Gibaud A (1999) X-Ray and neutron reflectivity: principles and applications. Springer, Berlin

Deibler GE, Martenson RE, Kies MW (1972) Large-scale preparation of myelin basic protein from central nervous tissue of several mammalian species. Prep Biochem 61:897–946

Deibler GE, Boyd LF, Kies MW (1984) Proteolytic activity associated with purified myelin basic protein. In: Alvord EC Jr, Kies MW, Suckling AJ (eds) Experimental allergic encephalomyelitis: a useful model for multiple sclerosis. Liss, New York pp 249–256

Facci P, Cavatorta P, Cristofolini L, Fontana MP, Fasano A, Riccio P (2000) Kinetic and structural study of the interaction of myelin basic protein with dipalmitoylphosphatidyl-glycerol layers. Biophys J 78:1413–1419

Gow A, Smith RJ (1989) The thermodynamically stable state of myelin basic protein in aqueous solution is a flexible coil. Biochem J 257:535–540

Graf K, Baltes H, Ahrens E, Helm CA, Husted CA (2002) Structure of hydroxylated galactocerebrosides from myelin at the air–water interface. Biophys J 82:896–907

Haas H, Torrielli M, Steitz R, Cavatorta P, Sorbi R, Fasano A, Riccio P, Gliozzi A (1998) Myelin model membranes on solid substrates. Thin Solid Films 327–328:627–631

Haas H, Oliveira CLP, Torriani IL, Polverini E, Fasano A, Carlone G, Cavatorta P, Riccio P (2004) Small angle X-ray scattering from lipid-bound myelin basic protein in solution. Biophys J 86:455–460

Harauz G, Ishyiama N, Hill CMD, Bates JR, Libich DS, Farès C (2004) Myelin basic protein-diverse conformational states of an intrinsically unstructured protein and its roles in myelin assembly and multiple sclerosis. Micron 35:503–542

Harper PE, Gruner SN, Lewis RNAH, McElhaney RN (2000) Electron density modeling and reconstruction of infinite periodic minimal surfaces (IPMS) based phases in lipid–water systems. Eur Phys J E 2:229–245

Hu Y, Douvedski I, Wood D, Moscarello M, Husted C, Genain C, Zasadzinski JA, Israelvichvili J (2004) Synergistic interactions of lipids and myelin basic protein. Proc Natl Acad Sci 101:13466–13471

Kaganer VM, Moehwald H, Dutta P (1999) Structure and phase transitions in Langmuir monolayers. Rev Mod Phys 71:779–819

Kirschner DA, Ganser L (1980) Compact myelin exists in the absence of basic protein in the shiverer mutant mouse. Nature 283:207–210

Kjaer K, Als-Nielsen J, Helm CA, Tippman-Krayer P, Mowald H (1989) Synchrotron X-ray diffraction and reflection studies of arachidic acid monolayers at the air–water interface. J Phys Chem 93:3200–3206

Konovalov O, Myagkov I, Struth B, Lohner K (2002) Lipid discrimination in phospholipid monolayers by the antimicrobial frog skin peptide PGLa. A synchrotron X-ray grazing incidence and reflectivity study. Eur Biophys J 31:428–437

Konovalov O, Struth B, Smilgies DM (2004) Troika II (ID10B): a versatile beamline for studies of liquid and solid interfaces. In: Warwick et al (eds) AIP conference proceedings No. 705, synchrotron radiation instrumentation: eighth international conference, pp352–355

Liebes LF, Zand R, Phillips WD (1975) Solution behavior, circular dichroism and 22 HMz PMR studies of the bovine myelin basic protein. Biochim Biophys Acta 405:27–39

Majewski J, Khul TL, Kjaer K, Smith GS (2001) Packing of ganglioside-phospholipid monolayers: an X-ray diffraction and reflectivity study. Biophys J 81:2707–2715

Martenson RE (1992) Myelin: biology and chemistry. CRC Press, Boca Raton

Mueller H, Butt HJ, Bamberg E (1999) Force measurements on myelin basic protein adsorbed to mica and lipid bilayer surfaces done with the atomic force microscope. Biophys J 76:1072–1079

Mueller H, Butt HJ, Bamberg E (2000) Adsorption of membrane-associated proteins to lipid bilayers studied with an atomic force microscope: myelin basic protein and cytochrome. J Phys Chem B 104:4552–4559

Nevot L, Croce P (1980) Caractérisation des surfaces par réflexion rasant de rayons x: application á l'étude du polissage de quelques verres silicates. Rev Phys Appl 15:761–779

Ohler B, Graf K, Bragg R, Lemons T, Coe R, Genain C, Israelachvili J, Husted C (2004) Role of lipid interactions in autoimmune demyelination. Biochim Biophys Acta 1688:10–17

Parratt LG (1954) Surface studies of solids by total reflection of X-rays. Phys Rev 95:359–369

Polverini E, Fasano A, Zito F, Riccio P, Cavatorta P (1999) Conformation of bovine myelin basic protein purified with bound lipids. Eur Biophys J 28:351–355

Polverini E, Arisi S, Cavatorta P, Berzina T, Cristofolini L, Fasano A, Riccio P, Fontana MP (2003) Interaction of myelin basic protein with phospholipid monolayers: mechanism of protein penetration. Langmuir 19:872–877

Riccio P, Masotti L, Cavatorta P, De Santis A, Juretic D, Bobba A, Pasquali-Ronchetti I, Quagliariello E (1986) Myelin basic protein ability to organize lipid bilayers: structural transition in bilayers of lysophosphatidylcholine micelles. Biochem Biophys Res Commun 134:313–319

Roach A, Takahashi N, Pravtcheva D, Ruddle F, Hood L (1985) Chromosomal mapping of mouse myelin basic protein gene and structure and transcription of the partially deleted gene in shiverer mutant mice. Cell 42:149–155

Roberts G (1990) Langmuir–Blodgett films. Plenum Press, New York

Schwartz DK (1997) Langmuir–Blodgett film structure. Surf Sci Rep 27:245–334

Smith R (1992) The basic protein of CNS myelin: its structure and ligand binding. J Neurochem 59:1589–1608